Article

TSFZ Growth of Eu-Substituted Large-Size LSCO Crystals

Olesia Voloshyna [1,*], Vitaliy V. Romaka [2], Koushik Karmakar [3], Silvia Seiro [1], Andrey Maljuk [1] and Bernd Büchner [1]

[1] Leibniz IFW Dresden, Helmholtzstr. 20, 01069 Dresden, Germany; s.seiro@ifw-dresden.de (S.S.); a.malyuk@ifw-dresden.de (A.M.); b.buechner@ifw-dresden.de (B.B.)

[2] Technische Universität Dresden, Bereich Mathematik und Naturwissenschaften, Fakultät Chemie und Lebensmittelchemie, Helmholtzstr. 10, 01069 Dresden, Germany; vitaliy.romaka@tu-dresden.de

[3] Helmholtz-Zentrum Berlin für Materialien und Energie, Hahn-Meitner-Platz 1, 14109 Berlin, Germany; koushik.karmakar@helmholtz-berlin.de

* Correspondence: o.voloshyna@ifw-dresden.de

Abstract: The travelling solvent floating zone (TSFZ) growth of Eu-substituted LSCO ($La_{1.81-x}Eu_xSr_{0.19}CuO_4$, with nominal $x = 0 \div 0.4$) single crystals was systematically explored for the first time. The substitution of La with Eu considerably decreased the decomposition temperature. Optimal growth parameters were found to be: oxygen pressure 9.0–9.5 bars; Eu-free CuO-poor solvent (66 mol% CuO) with a molar ratio of La_2O_3:$SrCO_3$:CuO = 4:4.5:16.5 and growth rate 0.6 mm/hour. The obtained single crystals were characterized with optical polarized microscopy, X-ray diffraction and energy-dispersive X-ray spectroscopy analysis. The solubility of Eu in LSCO appeared to be limited to x~0.36–0.38 under the used conditions. The substitution of La^{3+} with smaller Eu^{3+} ions led to a structural transition from tetragonal with space group *I4/mmm* for $La_{1.81}Sr_{0.19}CuO_4$ (x = 0) to orthorhombic with space group *Fmmm* for $La_{1.81-x}Sr_{0.19}Eu_xCuO_4$ (x = 0.2, 0.3, 0.4), and to a substantial shrinking of the c-axis from 13.2446 Å (x = 0.0) to 13.1257 Å (x = 0.4). Such structural changes were accompanied by a dramatic decrease in the superconducting critical temperature, Tc, from 29.5 K for x = 0 to 13.8 K for 0.2. For $x \geq 0.3$, no superconductivity was detected down to 4 K.

Keywords: travelling solvent floating zone; X-ray diffraction; cuprates; superconducting materials

1. Introduction

Despite over three decades of intense research, high-Tc superconducting cuprates remain a focus of investigation. The nature of the so-called pseudogap phase existing at temperatures above Tc and its suppression at a critical doping p^* close to where Tc reaches its maximal value is still being actively studied in Nd- and Eu-substituted $La_{2-y}Sr_yCuO_4$ (LSCO) [1–3]. The substitution of La^{3+} with Sr^{2+} allows to systematically vary the doping, while the substitution of a fixed fraction of La^{3+} with smaller Nd^{3+} or Eu^{3+} lowers Tc and increases p^*, increasing the range of observation of the pseudogap phase. In contrast, the evolution of the physical properties at fixed doping upon the systematic substitution of La^{3+} with isovalent smaller cations, akin to a chemical pressure, has received less attention. Growth conditions for Nd- or Eu-substituted LSCO in the literature are rarely given, mainly referring to those of rare-earth-free LSCO crystals [4–6]. An exception is a report on the crystal growth of $La_{1.6-y}Nd_{0.4}Sr_yCuO_4$ in air using a 78 mol% CuO, which claims that growth speeds higher than 1 mm/h dramatically affect the crystal quality, 0.65 mm/h yielding optimal results [7]. Recently, we showed that the growth of $La_{1.81-x}Nd_xSr_{0.19}CuO_4$ with the TSFZ technique using a copper-rich solvent (78–80 CuO mol%), as routinely employed for x = 0 but with the appropriate ratio of Nd, La and Sr, for $x \geq 0.2$ led to a considerable amount of bubbles in the molten zone (produced by the reduction in CuO with the release of oxygen gas) and introduced large voids in the grown ingots, which presented a poor crystallinity [8]. We could considerably suppress the bubbling and improve the quality of the Nd-substituted crystals by reducing the copper content of the solvent to

65–66 mol%, increasing the oxygen pressure to 5.5–6.5 bar and decreasing the growth rate to 0.6 mm/h.

The Eu^{3+} ion possesses a smaller ionic radius (0.947 Å) than Nd^{3+} (0.983 Å), potentially allowing for a larger chemical pressure effect at similar substitution levels. Changing the nature of the substituting ion, however, can influence not only the properties of the solid, but also the liquidus temperature, the solubility, the viscosity and the reactivity of the melt, requiring a further optimization of the growth parameters. We show that the crystals grown using the optimal growth parameters found for Nd-substituted LSCO, although intact on the border, present a considerable amount of decomposition at the core. This effect becomes more marked upon increasing the Eu content, but could be suppressed by using an Eu-free solvent and increasing the oxygen pressure to 9–9.5 bar. Eu-substituted crystals present an orthorhombic (*Cmce*) structure instead of a tetragonal (*I4/mmm*) one of LSCO, and the volume per formula unit decreases with x, accompanied by a rapid decrease in Tc.

2. Materials and Methods

Powders of La_2O_3 (ChemPUR Feinchemikalien und Forschungsbedarf GmbH, Karlsruhe, Germany), Eu_2O_3, CuO and $SrCO_3$ (Alfa Aesar by Thermo Fisher Scientific GmbH, Kandel, Germany) with a purity of no less than 4N were used as starting materials in the preparation of feed-rods and solvents. The procedure for raw material synthesis as well as for the production of feed rods was similar to that described in [8], using the same precursor ratios with Eu_2O_3 instead of Nd_2O_3. In particular, a Cu-rich solvent (78–80 mol% CuO) was prepared from a molar ratio of La_2O_3:Eu_2O_3:$SrCO_3$:CuO of 3:1:3.3:26, while for the Cu-poor solvent (65–66 mol% CuO), we used a 3.5:1:4:16.5 ratio. A small amount (3 wt%) of boron oxide was added in order to suppress the penetration of the solvent into the feed rod and the "swollen effect", as well as to increase the melt viscosity [9].

We observed that the substitution of La with Eu in LSCO led to a decrease in its decomposition temperature, to a more dramatic extent than the substitution with Nd. Therefore, the sintering temperature for Eu-LSCO was reduced to 1100 °C, compared to 1200 °C used for Nd-LSCO [8]. Unfortunately, decreasing the sintering temperature also led to a substantial decrease in the feed-rod density, which tended to favor the penetration effect and was detrimental for the stability of the TSFZ growth.

Crystals were grown on a four-mirror-type image floating zone furnace (CSC, Hokuto, Yamanashi, Japan) equipped with 300 W halogen lamps as the radiation source. The following conditions were used during the growth experiments: (i) feed and seed shafts rotated oppositely at 20 rpm; (ii) growth rates of 0.6–1.0 mm/h; (iii) oxygen atmosphere with pressure up to 9.5 bars.

Powder X-ray diffraction (XRD) measurements on crushed crystals were carried out at room temperature using an automated powder STOE Stadi P Dual Source diffractometer with Cu $K_{\alpha 1}$ radiation and a MYTHEN 2K detector. Data were collected in the 2θ range from 5° to 100.25° in 0.015° steps. The Rietveld analysis [10] was performed with a FullProf program package [11]. The space groups *I4/mmm* and *Cmce*, as well as the atomic positions published for $La_{1.85}Sr_{0.15}CuO_4$ [12] and $La_{1.94}Sr_{0.06}CuO_4$ [13], were used in the refinement.

Photographs for cross-sections of the crystals were obtained on a Zeiss Axiovert 25 Invert microscope in polarized light. The chemical composition was analyzed by means of energy-dispersive X-ray spectroscopy in a Zeiss EVOMA15 scanning electron microscope. The operating voltage was 30 kV. The La and Eu contents were determined using M- and L-lines, and for Cu and Sr contents, L- and K-lines were used.

Magnetization measurements were performed in a SQUID-VSM (Quantum design Germany, Darmstadt, Germany). A field of 50 Oe was applied in arbitrary directions for all the crystals.

3. Results and Discussion

3.1. Crystal Growth

In analogy to our previous findings for Nd-LSCO [8], growth experiments on Eu-LSCO crystals for x = 0.2 using a Cu-rich solvent and oxygen pressure in the range of 1–2 bar, as routinely used for LSCO, yielded poor results. As mentioned above, the relatively low sintering temperature resulted in a lower feed-rod density for Eu-substituted LSCO (compared to that of LSCO or even Nd-substituted LSCO). This in turn caused intense liquid penetration from the molten zone (MZ) into the feed-rod ("swallowing"), which led to a complete interruption of the growth.

As we had previously shown, using a CuO-poor solvent with 65–66 mol% CuO in the growth of Nd-LSCO efficiently suppressed the penetration of the solvent from the MZ into the feed rod [8]; therefore, we used an analogous solvent with a $La_2O_3:Eu_2O_3:SrCO_3:CuO$ ratio of 3.5:1:4:16.5 to counteract the influence of the low density of feed rods on the growth stability of Eu-LSCO. This resulted in a very stable growth run for x = 0.2 at a pulling rate of 0.6 mm/h and 5.5–6.5 bar oxygen pressure, see Figure 1. The crystallization front exhibited a sinusoidal shape and facets could be observed in the grown crystal.
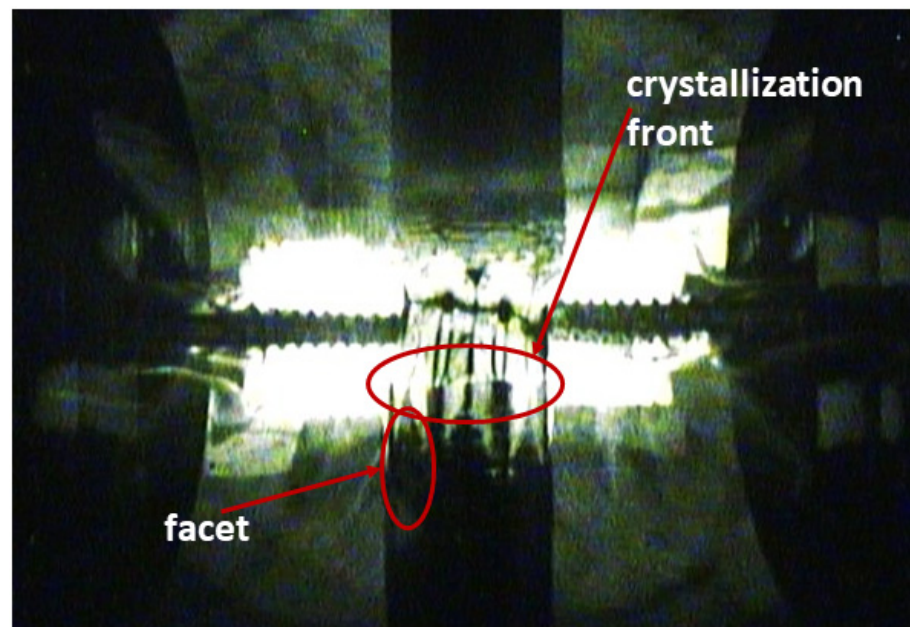

Figure 1. Image of the TSFZ growth of $La_{1.61}Sr_{0.19}Eu_{0.2}CuO_4$ using a Cu-poor solvent analogous to that used in Ref. [8].

In spite of a mirror-like surface with a metallic luster of the ingot, an image of its cross section in Figure 2 revealed a large number of voids and impurity phases in the central part of the crystal. Long straight streaks were observed, which the EDX analysis showed to consist of a mixture of La_2O_3 and Eu_2O_3, without Cu. Enclosed between such streaks were areas of composition consistent with the nominal one, as well as Cu-containing areas enriched in La or Eu. The composition in the border regions of the ingot was consistent with $La_{1.61}Sr_{0.19}Eu_{0.2}CuO_4$. This contrast between the border and the core of the ingot suggested that although the phase crystallized from the melt, decomposition occurred upon cooling after solidification.
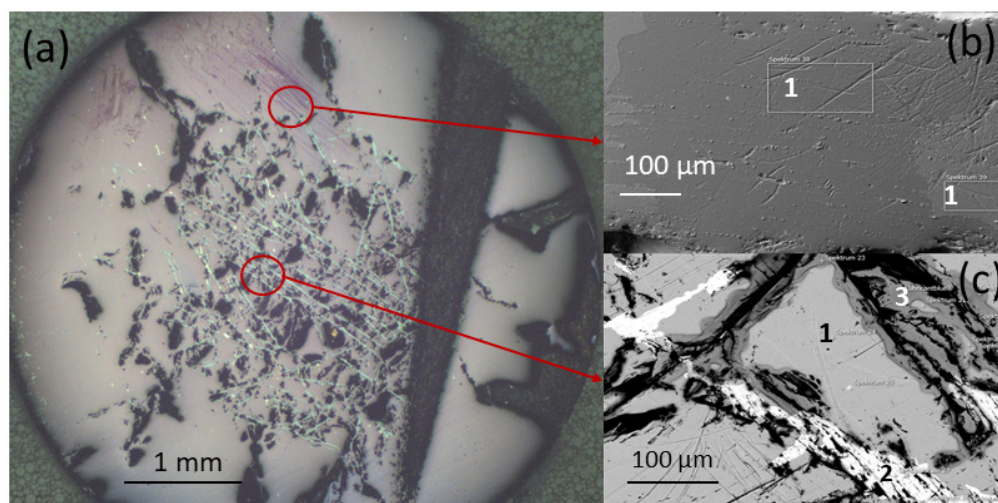
Figure 2. (**a**) Polarized microscopy photograph of the cross-section of a crystal with composition $La_{1.61}Sr_{0.19}Eu_{0.2}CuO_4$ grown from a solvent with precursor ratio (3.5:1:4:16.5). (**b**,**c**) SEM backscattered electron images corresponding to the areas marked on the left panel, where 1 indicates $La_{1.61}Eu_{0.2}Sr_{0.19}CuO_4$, 2 indicates areas consisting of La_2O_3 and Eu_2O_3 and 3 areas enriched in La or Eu.

In order to suppress this decomposition, we increased the growth rate from 0.6 mm/h to 0.8 mm/h and 1.0 mm/h. We expected that a faster growth rate would favor a rapid cooling of the crystal, avoiding decomposition. Figure 3 shows cross-sections of the grown ingot for different growth rates. Although a slight improvement was observed, even at 1 mm/h, such long streaks of secondary phases were still present.
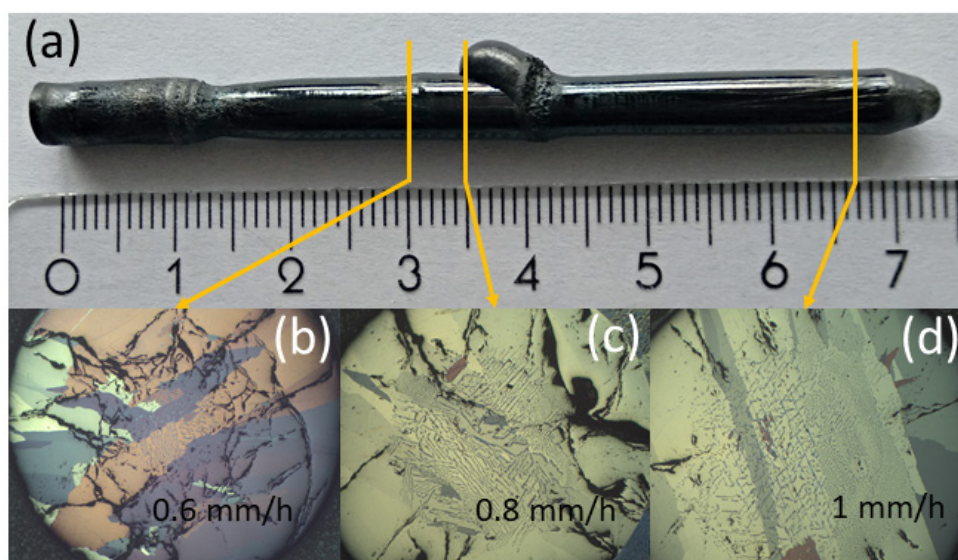

Figure 3. (**a**) Photo of the crystal with general composition $La_{1.51}Sr_{0.19}Eu_{0.3}CuO_4$, grown with different growth rates; (**b**–**d**) polarized microscopy photography of single crystal cross-sections, respective to a different growth rates, applied during the growth run.

In order to further favor a rapid cooling of the crystals, we applied a high oxygen pressure (9–9.5 bar instead of 5.5–6 bar, used for the growth of Nd-LSCO crystals [8]). As shown in Figure 4, such an increase in the oxygen pressure significantly reduced the crystal decomposition, but unfortunately did not avoid it completely.
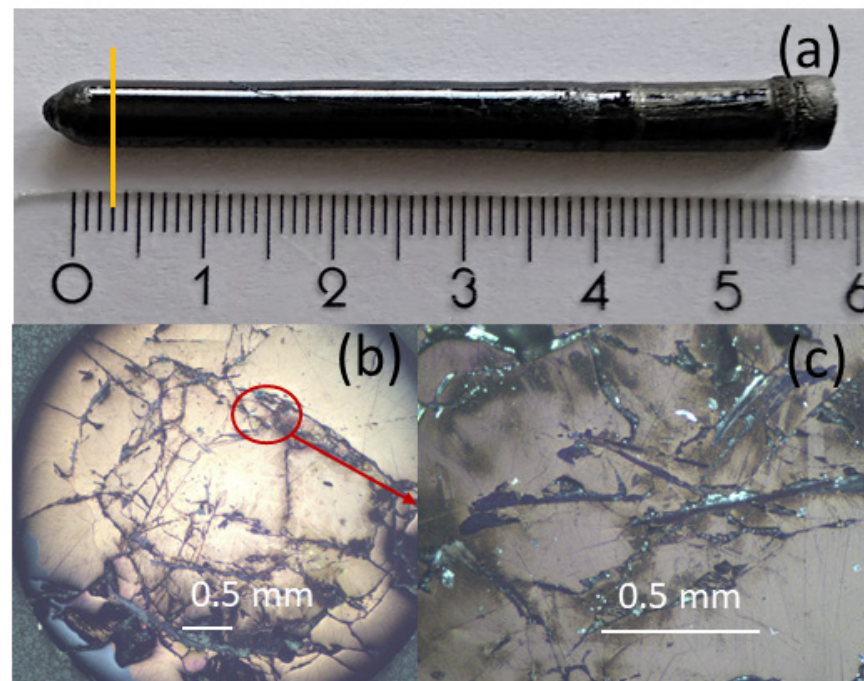
Figure 4. (**a**) Ingot of $La_{1.61}Sr_{0.19}Eu_{0.2}CuO_4$, grown at an oxygen pressure of 9 bar using Eu-containing solvent. The yellow line indicates the position of the cross section in (**b**). (**b**) Polarized microscopy photography of the cross section indicated in (**a**). The zone highlighted in red is shown at higher magnification in (**c**).

Since in the Eu-free LSCO such a inhomogeneity at the core of the ingots was not observed, it could be related to an excessive concentration of Eu_2O_3. As a next step, we removed all Eu_2O_3 from the solvent, using a "copper-poor" solvent with a molar ratio of $La_2O_3:SrCO_3:CuO = 4:4.5:16.5$. This led to a drastic improvement in the quality of the grown Eu-LSCO crystals (see Figure 5). In addition to possessing a surface with a metallic luster, cross-section cuts of x = 0.3 ingots as that in Figure 5a showed a homogeneous core, with only tiny occasional areas enriched in Sr or Eu present at grain boundaries only. The decomposition of the crystal after solidification was completely suppressed. The composition of the main phase corresponded to the nominal one: $La_{1.51}Sr_{0.19}Eu_{0.3}CuO_4$. This indicated that after an initial stage, when the MZ incorporated Eu from the feed, the MZ reached Eu-saturation and the composition stabilized, crystallizing the desired phase.

Using the determined optimal growth parameters, (i) oxygen pressure 9–9.5 bar and (ii) a "CuO-poor" Eu-free solvent with a molar ratio of $La_2O_3:SrCO_3:CuO = 4:4.5:16.5$, single crystals for Eu-substituted LSCO were obtained for different values of x = 0.2 ÷ 0.4. As shown in Figure 6, the obtained crystals (length up to 70 mm and 5–5.5 mm in diameter) exhibited a metal luster on the surface, while the single-crystal part of the ingots was up to 30 mm in length and up to 4.5 mm in diameter. The polarized microscopy of cross-sections of the end portions of the grown ingots for x = 0.2 and 0.3 showed a large main singe-crystal grain with some secondary grains close to the ingot border. The analysis with EDX confirmed the composition of the crystals to be $La_{1.61}Sr_{0.19}Eu_{0.2}CuO_4$ and $La_{1.51}Sr_{0.19}Eu_{0.3}CuO_4$, respectively.
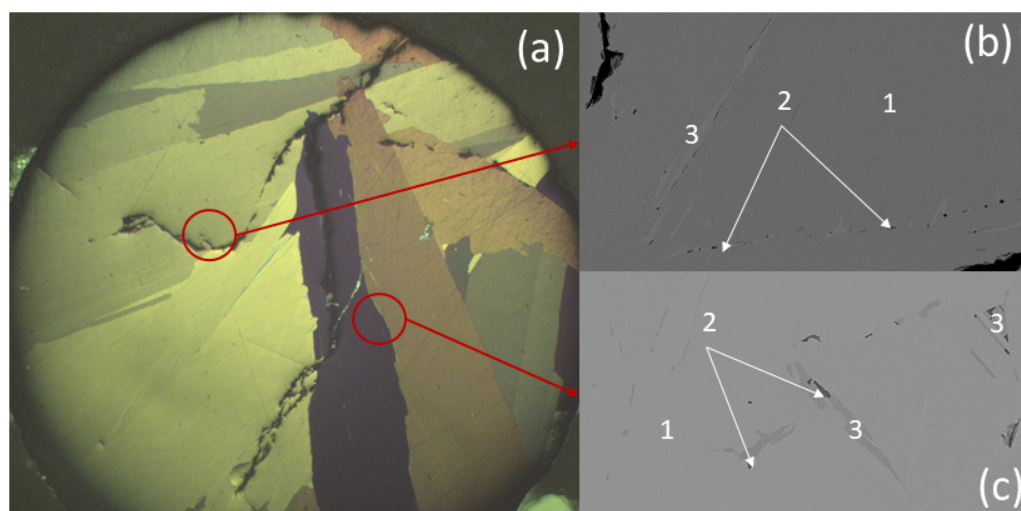
Figure 5. (**a**) Polarized microscopy image of a cross-section of $La_{1.51}Sr_{0.19}Eu_{0.3}CuO_4$ grown using Eu-free, Cu-poor solvent. (**b**,**c**) SEM backscattered electron images corresponding to the areas marked on the left panel, where: 1—$La_{1.51}Eu_{0.3}Sr_{0.19}CuO_4$; 2—areas enriched with Sr; 3—areas enriched with Eu.
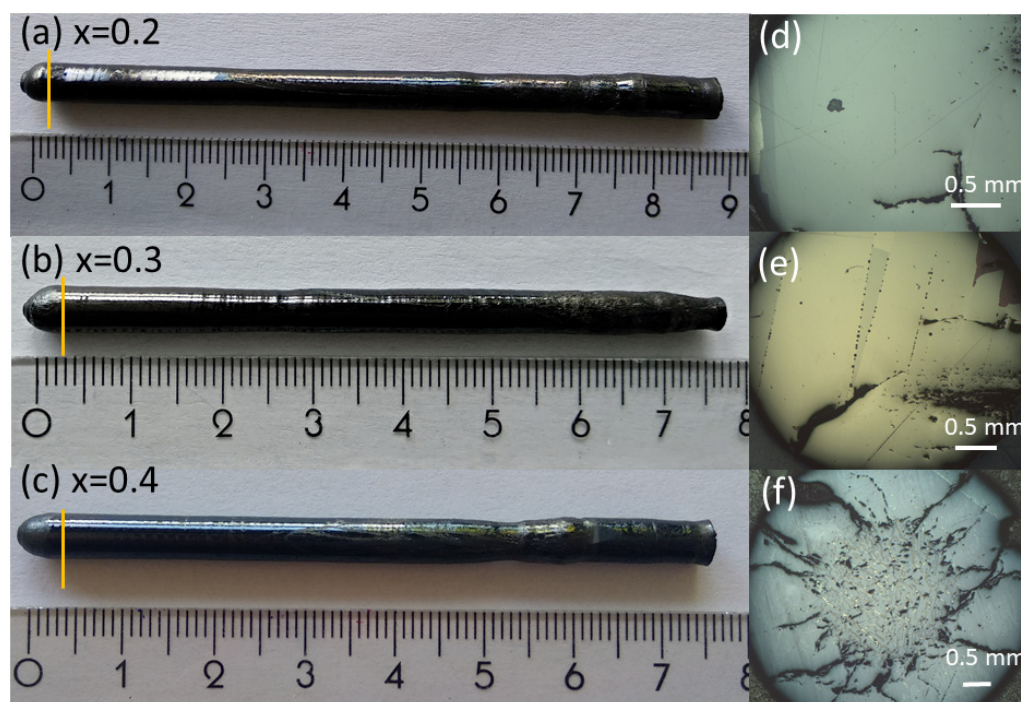

Figure 6. Grown crystals of nominal composition $La_{1.81-x}Sr_{0.19}Eu_xCuO_4$, $x = 0.2$ (**a**), $x = 0.3$ (**b**) and $x = 0.4$ (**c**) and their corresponding cross-sections (**d**–**f**).

For $x = 0.4$, however, decomposition in the central part of the crystal was still observed. This could be an indication that the solubility limit for Eu in LSCO lies in between $x = 0.3$ and $x = 0.4$. The EDX analysis performed on the surface in Figure 6f showed that the long whitish lines in the central part of the crystal consisted of lanthanum and europium oxides (La_2O_3 and Eu_2O_3), similarly to those observed in Figure 2. The EDX analysis on pieces taken from the border of the ingot proved that the actual Eu content of the crystal lies in the range $x = 0.36 \div 0.38$, which probably represents the Eu solubility limit in LSCO.

3.2. Structural Characterization

Powder XRD patterns of crushed crystals exhibited the presence of the expected $La_{1.81-x}Eu_xSr_{0.19}CuO_4$ phase, without any detectable traces of impurities.

The Rietveld analysis of the powder pattern for x = 0 confirmed that this compound crystallized in the K_2NiF_4-type structure (space group $I4/mmm$), often denoted as HTT (high-temperature tetragonal), in agreement with previous reports [12]. Two changes were observed upon increasing the Eu content: an overall shift of the peaks to higher diffraction angles, and a splitting of certain diffraction peaks (see Figure 7).
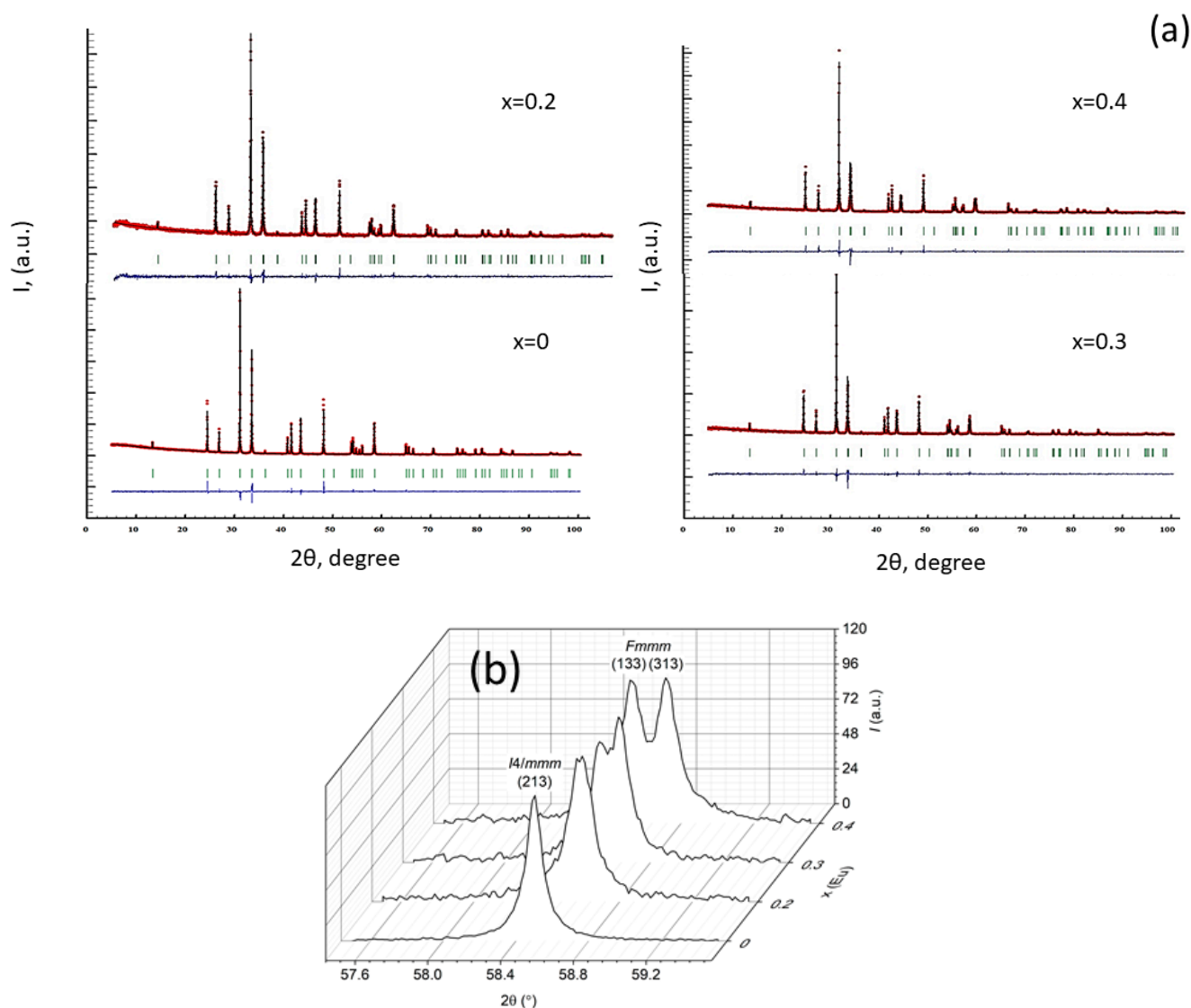

Figure 7. Diffraction patterns for $La_{1.81-x}Eu_xSr_{0.19}CuO_4$ (x = 0 ÷ 0.4) crystals (**a**) and splitting for diffraction peaks at 58.5° with increase in Eu content in $La_{1.81-x}Sr_{0.19}Eu_xCuO_4$ (x = 0 ÷ 0.4) single crystals (**b**).

Peak splitting is indicative of a symmetry reduction. All reflections of the Eu-substituted LSCO with nominal x = 0.4 were successfully indexed in the orthorhombic system and appeared to be similar to several structural modifications of the LSCO compound with orthorhombic space groups $Cmce$ [13] and $Fmmm$ [14]. The Rietveld refinement for all the Eu-substituted LSCO compounds was performed for both space groups, and showed that the space group $Fmmm$ was slightly favorable compared to $Cmce$, resulting in lower R_{Bragg} and especially R_F residuals, and significantly reduced standard deviations in atomic coordinates of the O1 atoms. In our XRD experiment, we did not detect additional reflections

that corresponded to the C-centering of the crystal lattice, due to their very low intensity. Moreover, a direct transition from the *I4/mmm* space group to *Cmce* was impossible and required an intermediate transfer through the space group *Fmmm*. This transition from *I4/mmm* to *Fmmm* was performed with the transformation of the *a* and *b* lattice vectors, resulting in the doubled volume of the unit cell (for more details, see Figure 8).
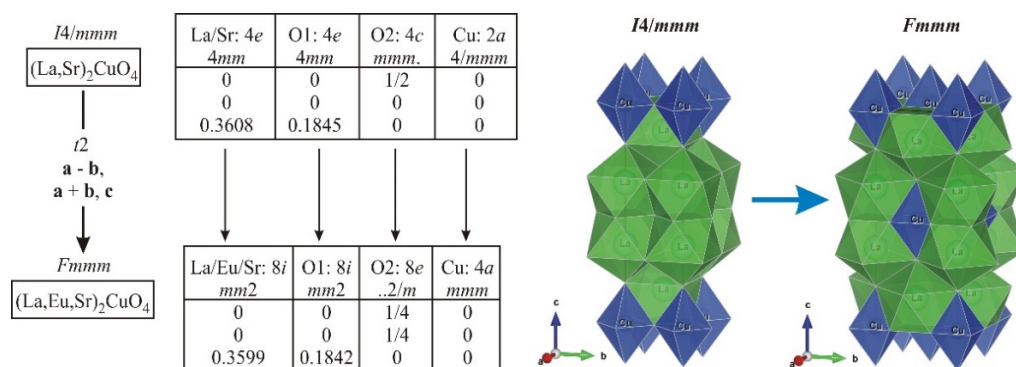
I4/mmm	La/Sr: 4*e* 4*mm*	O1: 4*e* 4*mm*	O2: 4*c* *mmm.*	Cu: 2*a* 4/*mmm*
$(La,Sr)_2CuO_4$	0	0	1/2	0
	0	0	0	0
	0.3608	0.1845	0	0

t2
a − b,
a + b, c

Fmmm	La/Eu/Sr: 8*i* *mm2*	O1: 8*i* *mm2*	O2: 8*e* ..2/*m*	Cu: 4*a* *mmm*
$(La,Eu,Sr)_2CuO_4$	0	0	1/4	0
	0	0	1/4	0
	0.3599	0.1842	0	0

I4/mmm　　　　*Fmmm*

Figure 8. Transition from *I4/mmm* to *Fmmm* in $La_{1.81-x}Sr_{0.19}Eu_xCuO_4$ (x = 0 ÷ 0.4) single crystals.

The volume per formula unit decreased with the increase in the Eu content, as expected, in view of the smaller ionic radius of Eu^{3+} with respect to that of La^{3+}. However, a linear dependence was observed only in the range $0.2 \leq x \leq 0.4$. The distance between the Cu–O planes changed linearly (decreasing by 0.9% between x = 0 and x = 0.4), while the average in-plane Cu–Cu distance remained basically unchanged (see Table 1). The substitution of La with Eu increased the mismatch between the rocksalt and the perovskite layers, favoring the orthorhombic structural distortion.

An analysis of the interatomic distances in the structures of Eu-substituted LSCO revealed, that among six oxygen atoms that formed an (O12O24) octahedron around each Cu atom, four O2 atoms (which formed a square in the pure LSCO in the ab plane) practically did not change their distances to Cu (d~0.1885 nm), despite a tiny deformation in this square for $x \geq 0.2$ due to the symmetry change. Two other O1 atoms somewhat decreased their distance to the Cu atom along the c-direction from 0.2444(8) nm in the pure LSCO to 0.2418(11) nm for x = 0.4. The distances from O2 to the La/Sr/Eu site also remained practically unchanged, while all contact distances between La/Sr/Eu and the O1 atoms decreased. This allowed us to conclude that the Cu–O2 layers were characterized by the strongest bonding, while the La/Sr/Eu-O1 framework was responsible for the lattice deformation while substituting.

These structural changes influenced the superconducting properties of Eu-substituted LSCO crystals. As it can be seen from Table 1, the superconducting Tc was detected for $La_{1.61}Sr_{0.19}Eu_{0.2}CuO_4$ only. For crystals with x = 0.3 and 0.4, no signature of superconductivity was detected down to 4 K. It is worth noting that the decrease in Tc between x = 0 and x = 0.2 was of roughly 50%, while for the Nd-substitution, the same decrease in Tc was obtained for x = 0.4.

Table 1. Summary of structural and superconducting information for Eu-LSCO.

Compound	$La_{1.81}Sr_{0.19}CuO_4$	$La_{1.61}Eu_{0.2}Sr_{0.19}CuO_4$	$La_{1.51}Eu_{0.3}Sr_{0.19}CuO_4$	$La_{1.41}Eu_{0.4}Sr_{0.19}CuO_4$
Refinement Data				
Space group, prototype	*I4/mmm* (#139), K_2NiF_4-type	*Fmmm* (#69), La_2CuO_4-type		
a, (b) c (Å)	3.7729(7), 13.245(1)	5.3256(4) 5.3339(0) 13.1820(1)	5.3244(3) 5.3393(8) 13.1483(3)	5.3197(3) 5.3435(7) 13.1257(9)
V (Å^3)	188.548(1)	374.454(4)	373.796(3)	373.118(3)
Reflections measured	45	68	68	68
$R_F = \Sigma \mid F_o\text{-}F_c \mid /\Sigma F_o$	0.0296	0.0735	0.0557	0.0486
$R_I = \Sigma \mid I_o\text{-}I_c \mid /\Sigma I_o$	0.0453	0.0649	0.0627	0.0419
$\chi^2 = (R_{wP}/R_e)^2$	1.86	1.77	1.89	2.18
Interatomic distances				
Cu-O1	0.2444(8)	0.2419(12)	0.2398(12)	0.2418(11)
Cu-O2	0.18864(1)	0.18844(1)	0.18851(1)	0.18850(1)
La/Sr/Eu-O1	0.27345(18)	0.2725(3)	0.2721(3)	0.2722(3)
La/Sr/Eu-O1	0.27345(18)	0.2729(3)	0.2729(3)	0.2734(3)
La/Sr/Eu-O1	2.336(9)	2.332(12)	2.342(12)	2.306(11)
La/Sr/Eu-O2	2.6374(7)	2.6338(11)	2.6302(10)	2.6334(9)
Superconducting temperature				
T_c, K	29.5	13.8	None (or lower than 4 K)	None (or lower than 4 K)

4. Conclusions

The growth of Eu-substituted LSCO ($La_{1.81-x}Eu_xSr_{0.19}CuO_4$, x = 0 ÷ 0.4) large-size crystals with the TSFZ method was investigated. Optimal growth conditions were determined: a Eu-free "CuO-poor" solvent with a molar ratio of La_2O_3:$SrCO_3$:CuO = 4:4.5:16.5, a pulling rate of 0.6 mm/h and 9.0–9.5 bar oxygen pressure. XRD and EDX analyses confirmed the phase purity of the crystals. The solubility limit of Eu in LSCO was found to be x~0.36–0.38. The substitution of the La^{3+} ion with smaller Eu^{3+} induced a structural transition from tetragonal (space group *I4/mmm*) for Eu-free LSCO to orthorhombic (space group *Fmmm*). The main effect of the substitution was to reduce the interplanar distance between the Cu–O planes, while the in-plane distances were only weakly affected. The superconducting Tc strongly decreased upon Eu substitution, with no transition detected down to 4 K for x = 0.3 and 0.4. The influence of the Eu substitution was much stronger than that of the Nd substitution, owing to the much smaller ionic size of Eu^{3+}.

Author Contributions: Conceptualization, B.B.; formal analysis, V.V.R.; investigation, O.V. and K.K.; writing—original draft preparation, O.V. and V.V.R.; writing—review and editing, A.M. and S.S.; supervision, A.M. and S.S.; project administration, B.B. All authors have read and agreed to the published version of the manuscript.

Institutional Review Board Statement: Not applicable.

Informed Consent Statement: Not applicable.

References

1. Doiron-Leyraud, N.; Cyr-Choinière, O.; Badoux, S.; Ataei, A.; Collignon, C.; Gourgout, A.; Dufour-Beauséjour, S.; Tafti, F.F.; Laliberté, F.; Boulanger, M.-E.; et al. Pseudogap phase of cuprate superconductors confined by Fermi surface topology. *Nat. Commun.* **2017**, *8*, 2044. [CrossRef]
2. Cyr-Choinière, O.; Daou, R.; Laliberté, F.; Collignon, C.; Badoux, S.; LeBoeuf, D.; Chang, J.; Ramshaw, B.J.; Bonn, D.A.; Hardy, W.N.; et al. Pseudogap temperature T* of cuprate superconductors from the Nernst effect. *Phys. Rev. B* **2018**, *97*, 064502. [CrossRef]
3. Michon, B.; Girod, C.; Badoux, S.; Kačmarčík, J.; Ma, Q.; Dragomir, M.; Dabkowska, H.A.; Gaulin, B.D.; Zhou, J.-S.; Pyon, S.; et al. Thermodynamic signatures of quantum criticality in cuprate superconductors. *Nature* **2019**, *567*, 218–222. [CrossRef] [PubMed]
4. Kojima, H.; Yamamoto, J.; Mori, Y.; Khan, M.K.R.; Tanabe, H.; Tanaka, I. Single crystal growth of superconducting $La_{2-x}M_xCuO_4$ (M = Ca, Sr, Ba) by the TSFZ method. *Physica C* **1997**, *293*, 14–19. [CrossRef]
5. Lee, C.-H.; Kaneko, N.; Hosoya, S.; Kurahashi, K.; Wakimoto, S.; Yamada, K.; Endoh, Y. Growth of large single crystals using the improved lamp-image floating-zone furnace: Application to $La_{2-x}Sr_xCuO_4$. *Supercond. Sci. Technol.* **1998**, *11*, 891–897. [CrossRef]
6. Tanaka, I.; Yamane, K.; Kojima, H. Single crystal growth of superconducting $La_{2-x}Sr_xCuO_4$ by the TSFZ method. *J. Cryst. Growth* **1989**, *96*, 711–715. [CrossRef]
7. Dragomir, M.; Ma, Q.; Clancy, J.P.; Ataei, A.; Dube, P.A.; Sharma, S.; Huq, A.; Dabkowska, H.A.; Taillefer, L.; Gaulin, B.D. Materials preparation, single-crystal growth, and the phase diagram of the cuprate high-temperature superconductor $La_{1.6-x}Nd_{0.4}Sr_xCuO_4$. *Phys. Rev. Mater.* **2020**, *4*, 114801. [CrossRef]
8. Voloshyna, O.; Karmakar, K.; Maljuk, A.; Romaka, V.V.; Blum, C.G.F.; Seiro, S.; Büchner, B. TSFZ growth of Nd-substituted LSCO superconducting crystals. *J. Cryst. Growth* **2021**, *562*, 126082. [CrossRef]
9. Maljuk, A.; Watauchi, S.; Tanaka, I.; Kojima, H. The effect of B_2O_3 addition on $La_{2-x}Sr_xCuO_4$ single-crystal growth. *J. Cryst. Growth* **2000**, *212*, 138–141. [CrossRef]
10. Rietveld, H.M. A profile refinement method for nuclear and magnetic Structures. *J. Appl. Cryst.* **1969**, *2*, 65–71. [CrossRef]
11. Rodriguez-Carvajal, J.; Roisnel, T. FullProf.98 and WinPLOTR: New Windows95/NT Applications for Diffraction. *Int. Union Crystallogr. Newsl.* **1998**, *20*, 35–36.
12. Wang, H.H.; Geiser, U.; Thorn, R.J.; Carlson, K.D.; Beno, M.A.; Monaghan, M.R.; Allen, T.J.; Proksch, R.B.; Stupka, D.L.; Kwok, W.K.; et al. Synthesis, structure, and superconductivity of single crystals of high $T_cLa_{1.85}Sr_{0.15}CuO_4$. *Inorg. Chem.* **1987**, *26*, 1190–1192. [CrossRef]
13. François, M.; Yvon, K.; Fischer, P.; Decroux, M. Structural phase transition at 150K in the high-temperature superconductor $La_{1.85}Sr_{0.15}CuO_4$. *Solid State Commun.* **1987**, *63*, 35–40. [CrossRef]
14. Radaelli, P.G.; Jorgensen, J.D.; Schultz, A.J.; Hunter, B.A.; Wagner, J.L.; Chou, F.C.; Johnston, D.C. Structure of the superconducting $La_2CuO_{4+\delta}$ phases ($\delta \approx 0.08, 0.12$) prepared by electrochemical oxidation. *Phys. Rev. B* **1993**, *48*, 499–510. [CrossRef] [PubMed]